CORRELATION OF THREE STANDARD SHEAR TESTS FOR UNIDIRECTIONAL GLASS-EPOXY COMPOSITES

By

H. Benson Dexter

Thesis submitted to the Graduate Faculty of the
Virginia Polytechnic Institute
in candidacy for the degree of

MASTER OF SCIENCE

in

ENGINEERING MECHANICS

June 1967

CORRELATION OF THREE STANDARD SHEAR TESTS FOR UNIDIRECTIONAL GLASS-EPOXY COMPOSITES

by

H. Benson Dexter

Thesis submitted to the Graduate Faculty of the

Virginia Polytechnic Institute

in candidacy for the degree of

MASTER OF SCIENCE

in

ENGINEERING MECHANICS

APPROVED:

Chairman, G. W. Swift

D. H. Pletta

H. F. Brinson

J. H. Sword

June 1967

Blacksburg, Virginia

II. TABLE OF CONTENTS

III. LIST OF TABLES AND FIGURES

IV. INTRODUCTION AND REVIEW OF LITERATURE

The demand for high strength, high stiffness, lightweight materials for aerospace applications has led to the use of filament reinforced composites, particularly high-strength glass filaments embedded in a relatively low-strength epoxy matrix material. Besides having high tensile strength-to-weight ratios, glass-epoxy composites exhibit adequate compressive properties for use in structural componets where compression is of primary interest. It has been shown that compressive failure of glass reinforced composites is due primarily to delamination between fibers and matrix (see refs. 1 and 2). The strength of glass-epoxy composites is highly dependent upon the transfer of load between adjacent fibers by resin shear. This mechanism of load transfer is commonly termed interlaminar shear, more so in laminates than in wound parts.

There is no commonly accepted method for determining shear strengths of glass-epoxy composites; consequently, considerable discrepancies in shear strengths determined by various methods have been noted in current literature (see refs. 3 and 4). It is possible that several methods for determining interlaminar shear strength can be utilized provided the test results are properly analyzed.

The purpose of this report is to show any possible correlation that exists for the shear strength of glass-epoxy composites as determined by three types of tests. The types of tests investigated were:
(1) Short beam interlaminar shear test similar to ASTM D 2344-65 T,

(2) saw-cut shear test similar to ASTM D 2345-65 T, and (3) torsion test on circumferentially wound cylinders.

An experimental shear modulus was determined from the stress-strain curves for each cylinder tested in torsion. The experimental values are compared with several existing elasticity solutions for predicting shear modulus of composite materials.

V. LIST OF SYMBOLS

ρ	density, lb/in^3
E	modulus of elasticity
μ	Poisson's ratio
V_f	ratio of volume of fibers to volume of composite
A	area, in^2
P	failure load, lb
t	thickness, in.
d_m	mean diameter of cylinder, in.
R_m	mean radius of cylinder, in.
T	failure torque, in-lb
τ	shear stress
γ	shear strain
G	shear modulus
G_{sec}	secant shear modulus
η	plasticity reduction factor
K_t	torsional buckling coefficient
Z	cylinder curvature parameter
L	length of cylinder between end fixtures, in.
D_i	flexural rigidity
B_i	extensional rigidity

Subscripts

f	glass fiber
avg	average
max	maximum
exp	experimental
x, y	coordinates
cr	critical

VI. EXPERIMENTAL INVESTIGATION

Specimen Fabrication

Short beams.- Glass-epoxy panels were fabricated by hot-pressing several layers of *Scotch-Ply XP-251 S, 12-inch-wide, pre-preg tape to form a unidirectional composite of desired thickness. The tape consisted of nonwoven S-glass impregnated with an epoxy resin. The constituent properties of the composite are shown in table 1. The composite was cured for 30 minutes at 300° F in a hot press under pressure of 30 psi. This combination of temperature and pressure was sufficient to remove most of the voids inherent in the composite. After a 30-minute cure under pressure, the panels were placed in an air-circulating oven at 300° F and postcured for 12 hours. After postcuring, short beams were cut from the panels so that the fibers were parallel to the length of the beam (see fig. 1(a)). The dimensions for the short beams cut from flat panels are shown in table 2(a). The dimensions shown are an average of several measurements.

The values for the volume fraction of glass fibers, V_f, listed in the tables were obtained from elevated temperature burnout tests. After the specimens were tested, some were subjected to a temperature of 1050° F for a period of 2-1/2 hours. This temperature and time was sufficient for virtually all the epoxy to sublimate. The remaining glass was weighed after burnout of the epoxy and converted to an equivalent volume fraction by using the density quoted in table 1. The average void content for the flat beams was approximately 3 percent.

*(3M designation)

Saw-cut shear specimens.- The saw-cut specimens were cut from the same panels as the short beams. Two parallel saw cuts were cut across the width of each specimen on opposite sides and through the depth a distance equal to one-half the thickness plus 0.005 inch. This insured that no filaments would be continuous throughout the length, thereby eliminating the possibility of a tensile failure of the middle laminae. A typical saw-cut specimen is shown in figure 2. The dimensions of the saw-cut specimens are shown in table 3. The distance between the inside of the saw cuts is also shown. The average void content for the flat beams was approximately 3 percent.

Circumferentially wound cylinders.- Glass-epoxy cylinders were circumferentially wound with *Scotch-Ply XP-249 S, 20 end pre-preg roving. Proper combination of winding tension and resin flow is required to produce low void content specimens. The cylinders fabricated for this investigation were made by winding several layers of pre-preg roving over a 3-inch-diameter sand mandrel with a winding tension of 7-1/2 pounds. The mandrel was constantly heated with a heat gun to approximately 200° F during the winding process to insure proper resin flow. Extra layers of glass were wound on the ends of the cylinders for gripping the specimens and to prevent end failures. After winding, the cylinders and mandrel were rotated in an air-circulating oven for 12 hours at 300° F. After curing the cylinders, the ends were cut parallel to each other and perpendicular to the length. The cylinders were then removed from the mandrel by washing the sand from the inside.

*(3M designation)

Aluminum end fixtures were bonded to the cylinders to enable attachment of the cylinders to the torsion machine (see fig. 3). Each cylinder had back-to-back strain rosettes diametrically opposite each other. The average void content for the five cylinders tested was approximately 1.0 percent. Dimensions for the five cylinders tested are shown in table 4.

After the cylinders had failed in torsion, arc segments with the dimensions shown in table 2(b) were cut from cylinders 4 and 5. A typical arc segment is shown in figure 1(b). The average void content for the arc segments was approximately the same as the void content for the cylinders.

Test Procedure

Short beam interlaminar shear tests.- The flat and arc segment beams were subjected to interlaminar shear tests as shown in figure 4. The span for these tests was 1/2 inch, and the span-to-depth ratio was chosen in such a manner to insure failure by horizontal shear rather than bending. The specimens were loaded with a 1/8-inch radius ram with a constant cross-head movement of 0.05 in./min until failure. Failure was identified when a sudden drop in load occurred. When the maximum load was reached, an interlaminar crack was produced in the specimen. Figure 5 shows typical cracks across the width of the flat and arc segment beams. The results of the test data are shown in tables 2(a) and 2(b).

Saw-cut shear tests.- The saw-cut specimens were tested in shear as shown in figure 6(a). Self-alining Templin grips were used to grip

the specimens with the jaws gripping 1 inch of the specimens at each end. The load was applied to the specimen at a constant cross-head rate of 0.05 in./min.

Since the specimens were not restrained from bending in the overlap or shear area, failure was caused by both tearing apart of the overlap and shearing in the plane of the overlap. The bending that takes place can be seen in figure 6(b) which was obtained just prior to failure of the specimen. Because of the stress concentration at the base of the saw cuts and the high tearing stresses present, the average failing stress is somewhat lower than the maximum shear stress expected. A typical failed specimen is shown in figure 6(c). The test results are shown in table 3.

Torsion test of cylinders.- Circumferentially wound cylinders were tested to failure in torsion to obtain maximum shear strengths. The cylinders were tested in a 60 000 in-lb capacity torsion machine in which one end of the cylinder was held fixed and the other end rotated to induce a torque. An overall and a closeup view of the torsion test apparatus is shown in figure 7. Torque-strain curves were monitored on an oscilloscope connected to various strain gages during the actual tests. The primary purpose of the oscilloscope was to observe the torque-strain curves as the test progressed. During loading, the strains and torque were recorded by the Langley Central Digital Data Recording Facility. The time interval of taking data ranged from 1 second to every 5 seconds. The test results for the cylinders tested are shown in table 4.

VII. TEST RESULTS AND DISCUSSION

Short Beams

Flat and arc segment beams were subjected to three-point bend tests to produce interlaminar shear failure. Elementary beam theory was used in calculating the maximum shear stresses in the beams at failure. A parabolic stress distribution was assumed and the maximum shear stresses shown in tables 2(a) and 2(b) were calculated using the relationship $\tau_{max} = 0.75\ P/A$, where P is the failure load and A is the cross-sectional area. An elasticity solution for the shear stresses in a rectangular beam subjected to three-point loading was investigated by Von Karman and Seewald (ref. 5). It was shown that the theoretical maximum shear stress occurs at $y = + t/4$ and was about 11 percent higher than the maximum shear stress obtained from elementary theory. The 11-percent difference represents the local effect near the point of application of load. Figure 8 shows typical shear stress distributions for flat beams subjected to three-point loading. The distributions shown were obtained by using the results presented in reference 6. Figure 8(a) shows that the maximum shear stress at $y = + t/4$ acts over a small portion of the span and the shear stress decreases very rapidly with increase in distance from the point of maximum shear stress. Elementary beam theory shows that the maximum shear stress occurs at $y = 0$ and acts over the entire span. Figure 8(b) shows essentially no increase in shear stress above that determined by elementary theory.

Some of the beams failed in interlaminar shear at $y = 0$ and some failed at $y = + t/4$. There was no direct correlation of failure load

with plane at which failure occurred. The stresses calculated for beams that failed at $y = 0$ were of the same order of magnitude as the stresses calculated for beams that failed at $y = t/4$. Shear failure in heterogenous materials could possibly be influenced by the presence of voids and weak planes; therefore, it is very difficult to precisely specify a particular plane of failure. Because the maximum shear stress at $y = t/4$ acts over a very small region it is believed that the maximum shear stress calculated using elementary theory at $y = 0$ is of more significance because it acts over the entire span.

Photomicrographs of cross sections of the short beams are shown in figure 5. The flat beams had a lower volume fraction of glass than the cylinder arc segments but the results shown in tables 2(a) and 2(b) are in close agreement. It is evident from figure 5 that the arc segments have closer filament packing than the flat beams. This is also shown in the calculated volume fractions of glass fibers shown in tables 2(a) and 2(b). Voids and "epoxy-rich" areas can also be seen in figure 5(a) and 5(b).

Saw-Cut Shear Specimens

When the saw-cut shear specimen is subjected to tensile loading, considerable bending is induced in the overlap as can be seen in figure 6(b). Calculation of the average shear stress by dividing the failure load by the shear area neglects the effect of bending and the stress concentration at the base of the saw cuts. Several investigators have studied a similar problem involving shear stresses in lap joints (see refs. 7, 8, and 9). Goland and Reissner's solution shows that the

major stress in the overlap is a "tearing stress" which tends to tear the overlap apart normal to the axis of loading. The shear stress has a maximum value very close to the edges of the overlap, but of a smaller magnitude than the tearing stress. This indicates that failure is initiated by tearing apart of the overlap. Tearing apart of the overlap was evidenced in the saw-cut shear specimens tested in the investigation reported herein. Just prior to failure of the specimens a splitting or tearing action took place at the base of each saw cut. Failure of the specimens took place soon after the initiation of tearing. Reference 4 shows the stress distribution between the saw cuts using the Goland and Reissner solution. Using the Goland and Reissner solution, as applied in reference 4, the maximum shear stress is approximately three to five times higher than the average shear stress for the saw-cut shear specimens tested in this investigation. To obtain an exact solution for the shear stress distribution in the saw-cut specimens an orthotropic elasticity problem must be solved.

Circumferentially Wound Cylinders

Circumferentially wound cylinders were subjected to uniform torsional loading to induce pure shear. The shear strengths shown in table 4 were calculated using the following relationship obtained from reference 10 for thin-walled tubes of circular cross section:

$$\tau = \frac{2T}{\pi d_m^2 t}$$

where τ is the maximum shear stress, T is the failure torque, d_m is the mean diameter of cylinder, and t is the cylinder wall thickness.

The maximum shear stress obtained for each cylinder is approximately the same except for cylinder 1 which is somewhat lower. Since the wall of cylinder 1 was thinner than the other cylinders, it is possible that torsional buckling could have caused a combined buckling and shear failure. An approximate torsional buckling stress for cylinder 1 is calculated in appendix A. It is shown that the calculated buckling stress is very close to the maximum shear stress at failure of the cylinder.

Shear stress-strain curves were obtained for each cylinder tested and are shown in figures 9(a) through 9(e). The experimentally determined values of shear modulus shown in table 4 are average values obtained from outside and inside stress-strain curves. A comparison between experimentally and analytically determined values of shear modulus for the cylinders tested in this investigation is shown in appendix B.

VIII. CORRELATION OF TEST RESULTS

To compare the results of each type of test, the shear strengths must be evaluated on an equal basis. The stresses for each type of specimen are induced according to the test method or geometry of the specimen. The short beam specimen is designed to fail in interlaminar shear by choosing a proper span-to-depth ratio. The saw-cut specimen fails in combined tearing and shear when subjected to tensile loading because of the geometry of the specimen. The circumferentially wound cylinders were designed to fail in pure shear when subjected to uniform torsional loading. None of the specimens were loaded in the same manner but each type of specimen was designed to fail in resin shear between the fibers. The short beams and cylinders failed in shear between fibers but failure of the saw-cut specimens was initiated by high tensile or tearing stresses normal to the plane of shear. The average shear strengths for the saw-cut specimens cannot be compared with the shear strengths of the beams and cylinders because of the high tearing stress. By comparing the results of tables 2 and 4, it is seen that the shear strengths of the beams and cylinders are in close agreement.

IX. CONCLUDING REMARKS

The shear strength of unidirectional glass-epoxy composites was investigated by three standard tests. The maximum shear strengths obtained from interlaminar shear tests of short beams and torsional tests of circumferentially wound cylinders are in very close agreement. The shear strengths obtained from saw-cut shear tests are low because of high tearing stresses in the overlap. The short beam interlaminar shear test and the torsion test of circumferentially wound cylinders are equally acceptable shear tests. The saw-cut shear specimen should not be used to determine maximum interlaminar shear strengths.

Shear moduli predicted by existing analytical solutions are in close agreement with experimental results.

X. ACKNOWLEDGMENTS

The author wishes to thank the National Aeronautics and Space Administration for the use of its facilities and for the opportunity to write this thesis while in its employment.

The author also wishes to thank Dr. George Swift, Engineering Mechanics Department, Virginia Polytechnic Institute, for his advice and interest in the preparation of this thesis. Thanks are also extended to , and for their assistance and advice during the course of this investigation.

The author also wishes to thank his wife, , who helped reduce the experimental data and plot the stress-strain curves.

XI. REFERENCES

1. Davis, John G., Jr., and Zender, George W.: Compressive Behavior of Plates Fabricated From Glass Filaments and Epoxy Resin. NASA TN D-3918, April 1967.

2. Broutman, L. J.: Failure Mechanisms for Filament Reinforced Plastics Subjected to Static Compression, Creep, and Fatigue. Proceedings, 19th Annual Tech. and Mgt. Conf., Reinforced Plastics Div., SPI, February 1964, Section 9-C.

3. Davis, J. William: Interlaminar Shear Testing of Filament Winding Materials. Proceedings, 19th Annual Tech. and Mgt. Conf., Reinforced Plastics Div., SPI, February 1964, Section 19-A.

4. Romstad, Karl: Methods for Evaluating Shear Strength of Plastic Laminates Reinforced With Unwoven Glass Fibers. Forest Products Laboratory, Forest Service, U.S. Dept. of Agriculture, FPL-033, May 1964.

5. Karman, T. V., and Seewald, F.: Abhandl. Aerodynam. Inst., Tech. Hochschule, Aachen, Vol. 7, 1927.

6. Timoshenko, S., and Goodier, J. H.: Theory of Elasticity. McGraw-Hill Book Co., Inc., 1951, pp. 99-105.

7. Goland, M., and Reissner, E.: The Stresses in Cemented Joints. Journal of Applied Mechanics, 1944, pp. A17-A27.

8. Sherrer, R. W.: Stresses in a Lap Joint With Elastic Adhesive. Forest Products Laboratory, Forest Service, U.S. Dept. of Agriculture. No. 1864, September 1957.

9. Cornell, R. W.: Determination of Stresses in Cemented Lap Joints. Journal of Applied Mechanics, Vol. 20, No. 3, 1953, pp. 355-364.

10. Shanley, F. R.: Strength of Materials. McGraw-Hill Book Co., Inc., 1957, pp. 484 and 485.

11. Gerard, George: Plastic Stability of Geometrically Orthotropic Plates and Cylindrical Shells. New York University Tech. Report SM 61-11, July 1961, pp. 14-15.

12. Hashin, Zvi, and Rosen, Walter B.: The Elastic Moduli of Fiber-Reinforced Materials. Journal of Applied Mechanics, Vol. 31E, June 1964, pp. 223-232.

13. Adams, Donald F., and Doner, Douglas R.: Longitudinal Shear Loading of a Unidirectional Composite. Journal of Composite Materials, Vol. 1, 1967, pp. 4-17.

14. Tsai, Stephen W.: Structural Behavior of Composite Materials. NASA CR-71, July 1964, Section 2, p. 6.

The vita has been removed from the scanned document

XIII. APPENDIXES

APPENDIX A

Torsional Buckling Analysis

The torsional buckling stress for orthotropic cylinders of moderate length can be calculated using the following equation obtained from reference 11:

$$\tau_{cr} = \frac{\eta K_t \pi^2 E_x t^2}{12\left(1 - \mu_x \mu_y\right)} \qquad \text{(A-1)}$$

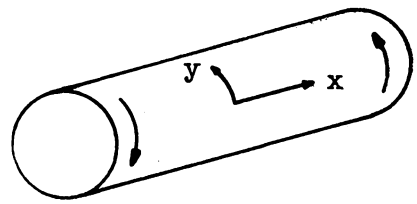

where the torsional buckling coefficient is

$$K_t = 0.764 \left(\frac{D_y}{D_x}\right)^{5/8} \left(\frac{B_x}{B_y}\right)^{3/8} \quad Z^{3/4} = 0.764\ Z_t{}^{3/4} \qquad \text{(A-2)}$$

Equation (A-2) applies for moderate length cylinders when $Z_t > 100$. The cylinder curvature parameter is computed from

$$Z = \left(\frac{B_y}{D_x}\right)^{1/2} \frac{L^2}{R_m t} \qquad \text{(A-3)}$$

The plasticity reduction factor in equation (A-1) is given by

$$\eta = \frac{G_{sec}}{G} \qquad \text{(A-4)}$$

The flexural and extensional rigidities are given by

$$D_x = \frac{E_x t^3}{12\left(1 - \mu_x \mu_y\right)} \quad , \quad D_y = \frac{E_y t^3}{12\left(1 - \mu_x \mu_y\right)}$$

and

$$B_x = \frac{E_x t}{1 - \mu_x \mu_y} \quad , \quad B_y = \frac{E_y t}{1 - \mu_x \mu_y}$$

The elastic constants for cylinder 1, obtained by using the equations in reference 12, are as follows:

$$E_x = 3.0 \times 10^6 \text{ psi} \quad , \quad E_y = 8.0 \times 10^6 \text{ psi}$$

$$\mu_x = 0.11 \quad , \quad \mu_y = 0.30$$

A length of 4.75 inches between the end fixtures was used in calculating the curvature parameter. The effect of the small taper on the ends of the cylinder was not considered in calculating the buckling stress.

The calculated critical shear stress using equation (A-1) is approximately 9100 psi. This is approximately 3 percent higher than the shear stress at failure of cylinder 1. For such a small difference, it is possible that the maximum shear stress obtained for cylinder 1 could have been influenced by buckling.

APPENDIX B

Comparison of Experimental and Analytical Shear Modulus

The shear modulus for each cylinder tested was calculated by three existing theories for predicting composite properties from constituent properties. Hashin and Rosen (ref. 12) obtained a solution for the shear modulus for a hexagonal array of fibers. The results shown in table 4 are for their upper-bound solution, which are consistently lower than the experimental results. Adams and Doner (ref. 13) used a finite difference technique to determine the shear modulus for a rectangular array of filaments embedded in an elastic matrix. Their results are in close agreement with the experimental results except for cylinder 3 which had a lower volume fraction of glass. Stephen Tsai (ref. 14) also obtained a solution which contains a contiguity factor where $C = 0$ implies that all filaments are isolated and $C = 1$ implies that the filaments are contiguous. It was recommended that a value of $C = 0.2$ be used for glass-epoxy composites. The values for shear modulus in table 4, obtained by using reference 14 for $C = 0.2$, are in very close agreement with the experimental results.

TABLE 1.- CONSTITUENT PROPERTIES* OF SPECIMENS

Material	ρ, lb/in^3	E, ksi	μ
S-901 Glass fiber	0.090	12 400	0.23
Epoxy	.0439	575	.42

*Data supplied by the Minnesota Mining and Manufacturing Company.

TABLE 2(a).- SHORT BEAM DIMENSIONS AND TEST RESULTS

Specimen (flat beam)	Thickness, in.	Width, in.	Length, in.	V_f	Failure load, lb	τ_{max}, psi
1	0.1406	0.2524	0.6353		463	9 785
2	.1433	.2498	.6359		515	10 790
3	.1464	.2491	.6331		494	10 160
4	.1481	.2487	.6346	0.556	512	10 426
5	.1456	.2485	.6357	.565	496	10 281
6	.1441	.2491	.6367	.570	500	10 447
7	.1460	.2487	.6329	.556	537	11 092
8	.1476	.2487	.6324	.547	460	9 398
9	.1451	.2484	.6355	.550	450	9 364
10	.1425	.2491	.6368	.547	473	9 994
11	.1415	.2502	.6325		480	10 168
12	.1433	.2500	.6333		504	10 551
13	.1409	.2518	.6349		477	10 084
14	.1435	.2526	.6345		500	10 345
15	.1485	.2503	.6360		478	9 645
16	.1392	.2526	.6354		535	11 411
17	.1385	.2521	.6365		543	11 664
18	.1403	.2533	.6360		515	10 869
19	.1385	.2488	.6351		514	11 187
20	.1376	.2521	.6361		528	11 416

TABLE 2(b).- SHORT BEAM DIMENSIONS AND TEST RESULTS

Specimen (arc segment)	Thickness, in.	Width, in.	Length, in.	V_f	Failure load, lb	τ_{max}, psi
4-1	0.0785	0.2449	0.6352	0.631	252	9 831
4-2	.0763	.2470	.6347	.642	263	10 466
4-3	.0753	.2488	.6339	.656	264	10 569
4-4	.0770	.2465	.6348	.642	257	10 155
5-1	.0793	.2535	.6321	.646	279	10 409
5-2	.0794	.2514	.6322	.643	267	10 032
5-3	.0774	.2496	.6324	.648	262	10 171
5-4	.0768	.2550	.6345	.653	254	9 727
5-5	.0784	.2503	.6342	.629	261	9 975
5-6	.0784	.2513	.6314	.629	270	10 278
5-7	.0778	.2518	.6311	.645	275	10 528
5-8	.0777	.2456	.6340	.636	257	10 100
5-9	.0778	.2489	.6302	.648	264	10 225
5-10	.0773	.2513	.6351	.650	272	10 502

TABLE 3.- SAW-CUT SPECIMEN DIMENSIONS AND TEST RESULTS

(Specimen length, 8.0 inches)

Specimen	Thickness, in.	Width, in.	Distance between saw cuts, in.	V_f	Failure load, lb	τ_{avg}
1	0.1498	0.9996	0.4848	0.565	1220	2518
2	.1471	.9997	.4819	.565	1200	2491
3	.1467	.9996	.4767		1230	2581
4	.1452	.9998	.4911	.567	1050	2138
5	.1441	1.0002	.4752	.567	935	1967
6	.1423	.9997	.4829	.572	1090	2258
7	.1416	.9996	.4878	.570	1125	2307
8	.1399	.9997	.4805	.568	1120	2332
9	.1394	.9948	.4788	.565	1090	2288
10	.1372	.9998	.4880		1245	2552

TABLE 4.- CYLINDER DIMENSIONS AND TEST RESULTS

(Cylinder: inside diameter, 3.0 in.; length 6.5 in.)

Cylinder	Thickness, in.	V_f	Failure torque, in-lb	τ_{max}, psi	G, psi $\times 10^6$			
					Exp.	Ref. 12	Ref. 13	Ref. 14
1	0.0460	0.624	5 890	8786	1.27	0.84	1.01	1.09
2	.0680	.633	9 500	9449	1.20	.87	1.03	1.12
3	.0664	.615	9 497	9684	1.25	.82	.90	1.07
4	.0782	.644	10 950	9408	1.18	.90	1.05	1.15
5	.0769	.645	11 100	9706	1.19	.91	1.07	1.15

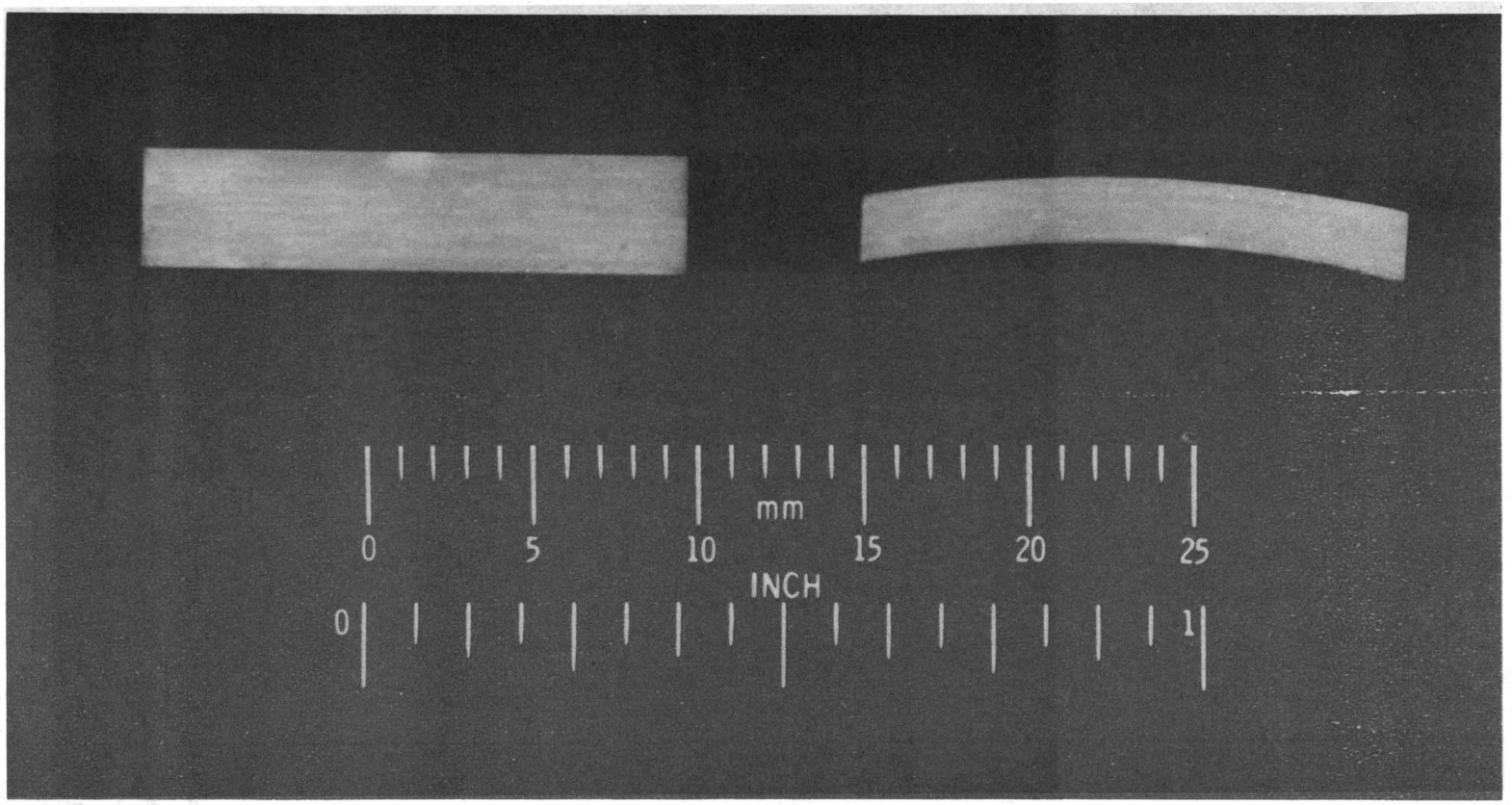

(a) Flat beam. (b) Cylinder arc segment.

Figure 1.- Short beam interlaminar shear specimens.

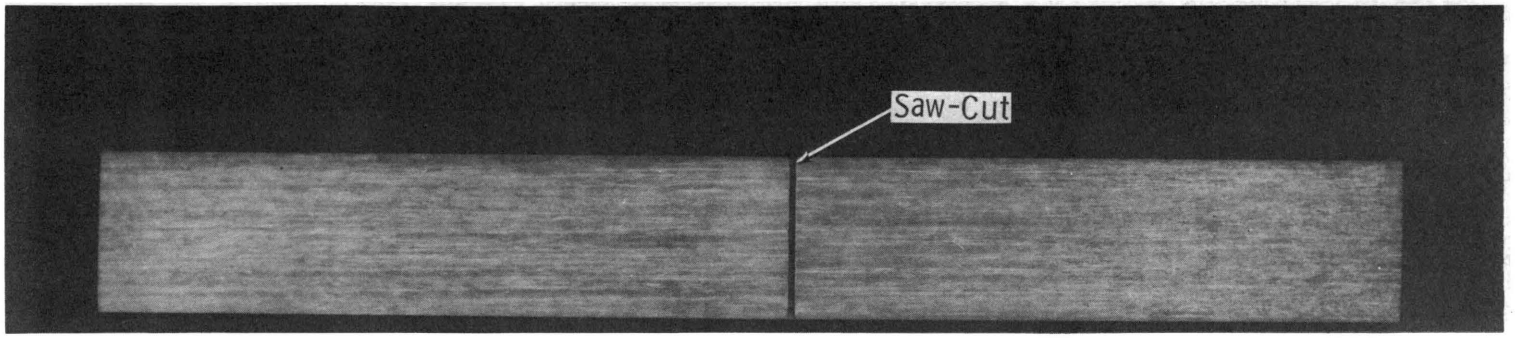

(a) Before test.

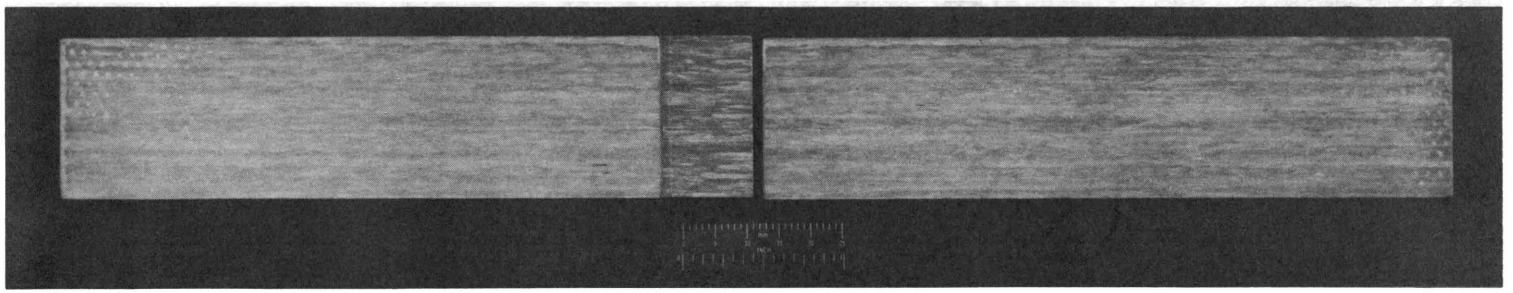

(b) After test.

Figure 2.- Saw-cut shear specimen before and after test.

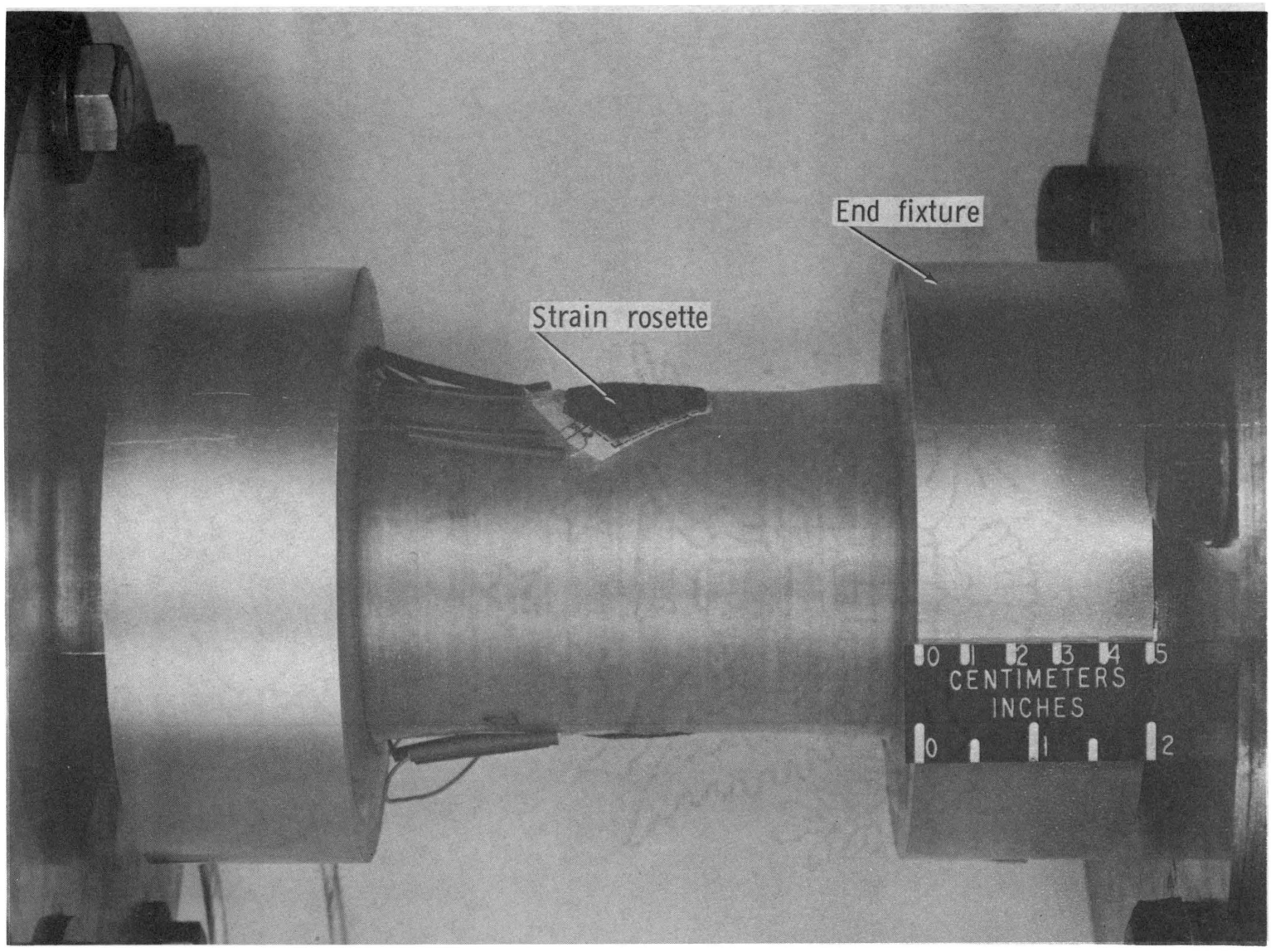

Figure 3.- Circumferentially wound glass-epoxy cylinder.

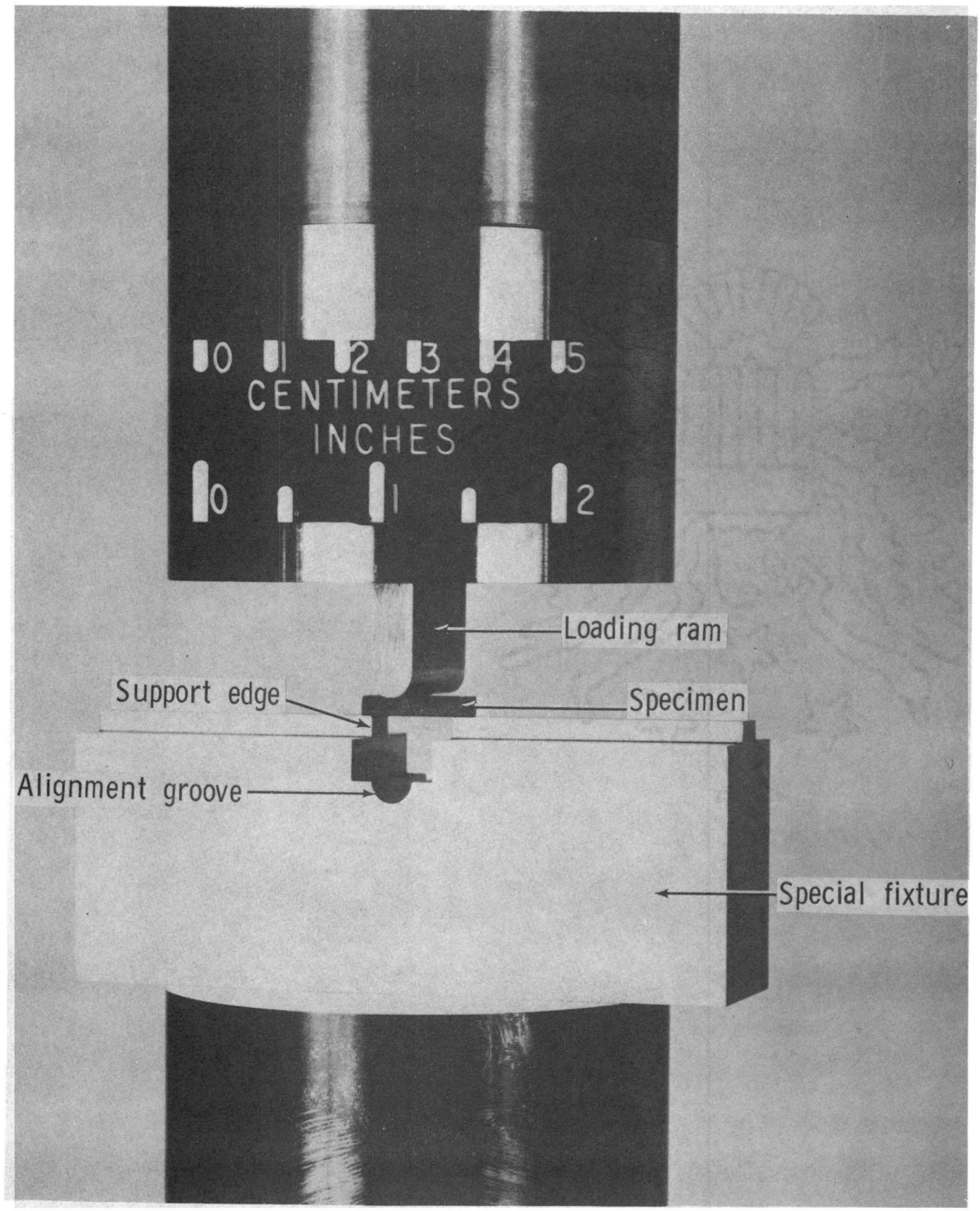

Figure 4.- Short beam interlaminar shear test fixture.

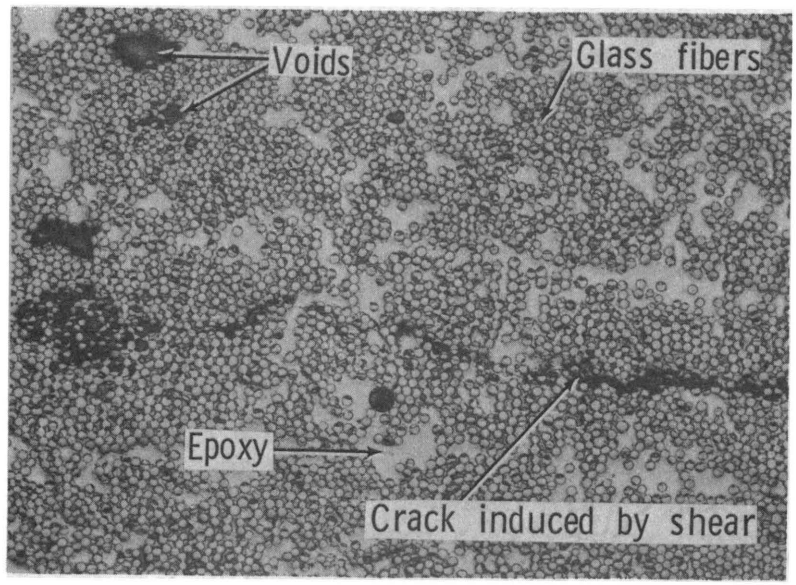

(a) Flat beam.

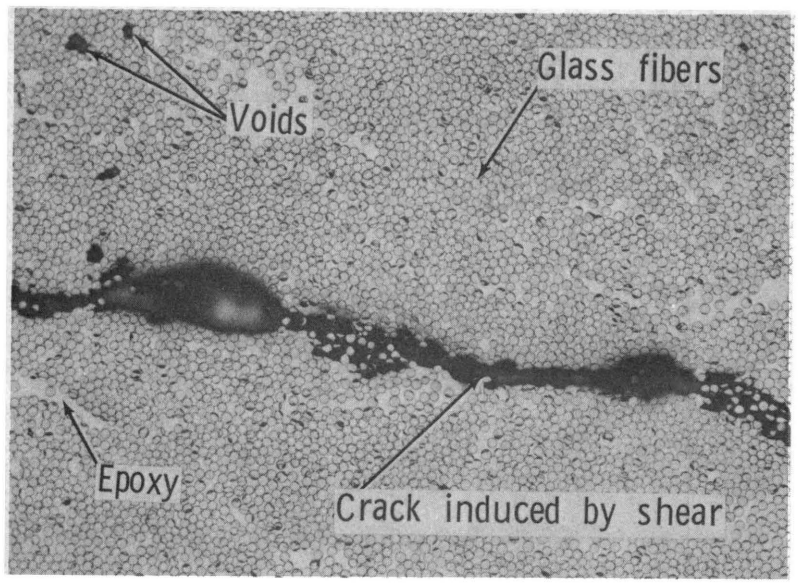

(b) Cylinder arc segment.

Figure 5.- Photomicrographs of short beam interlaminar shear specimens after test.

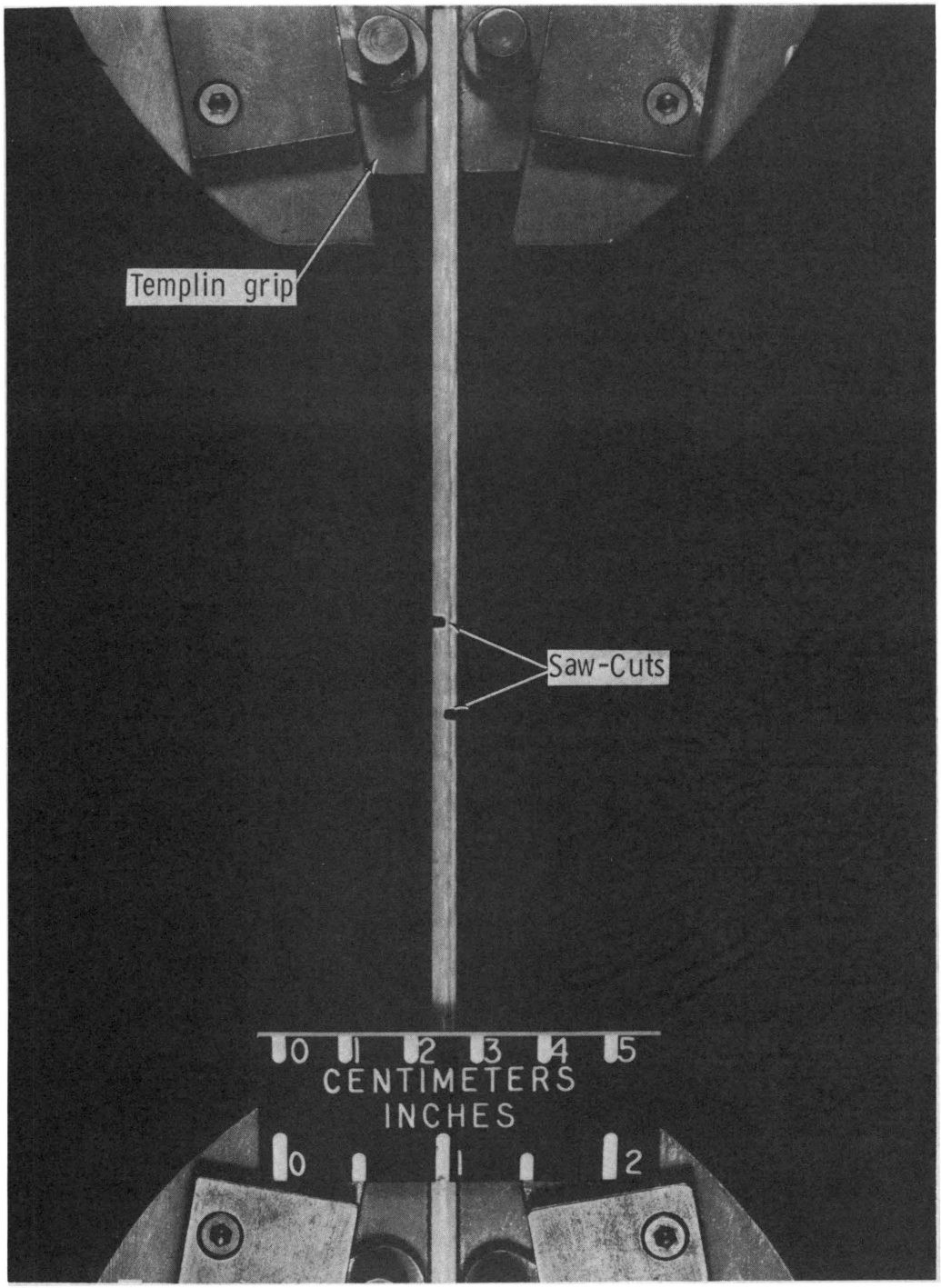

(a) Before test.

Figure 6.- Saw-cut shear specimen and loading fixture.

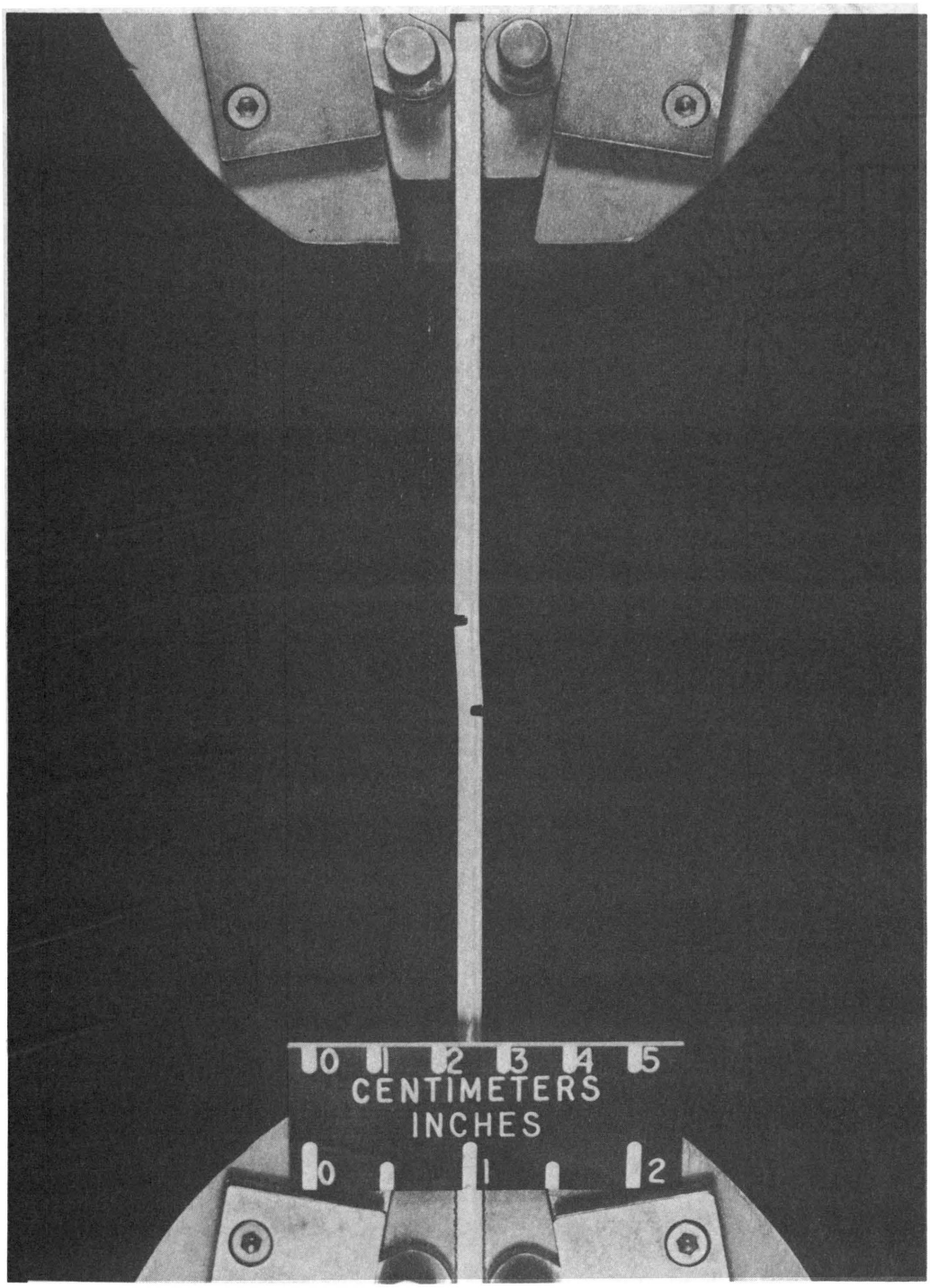

(b) Just prior to failure.

Figure 6.- Continued.

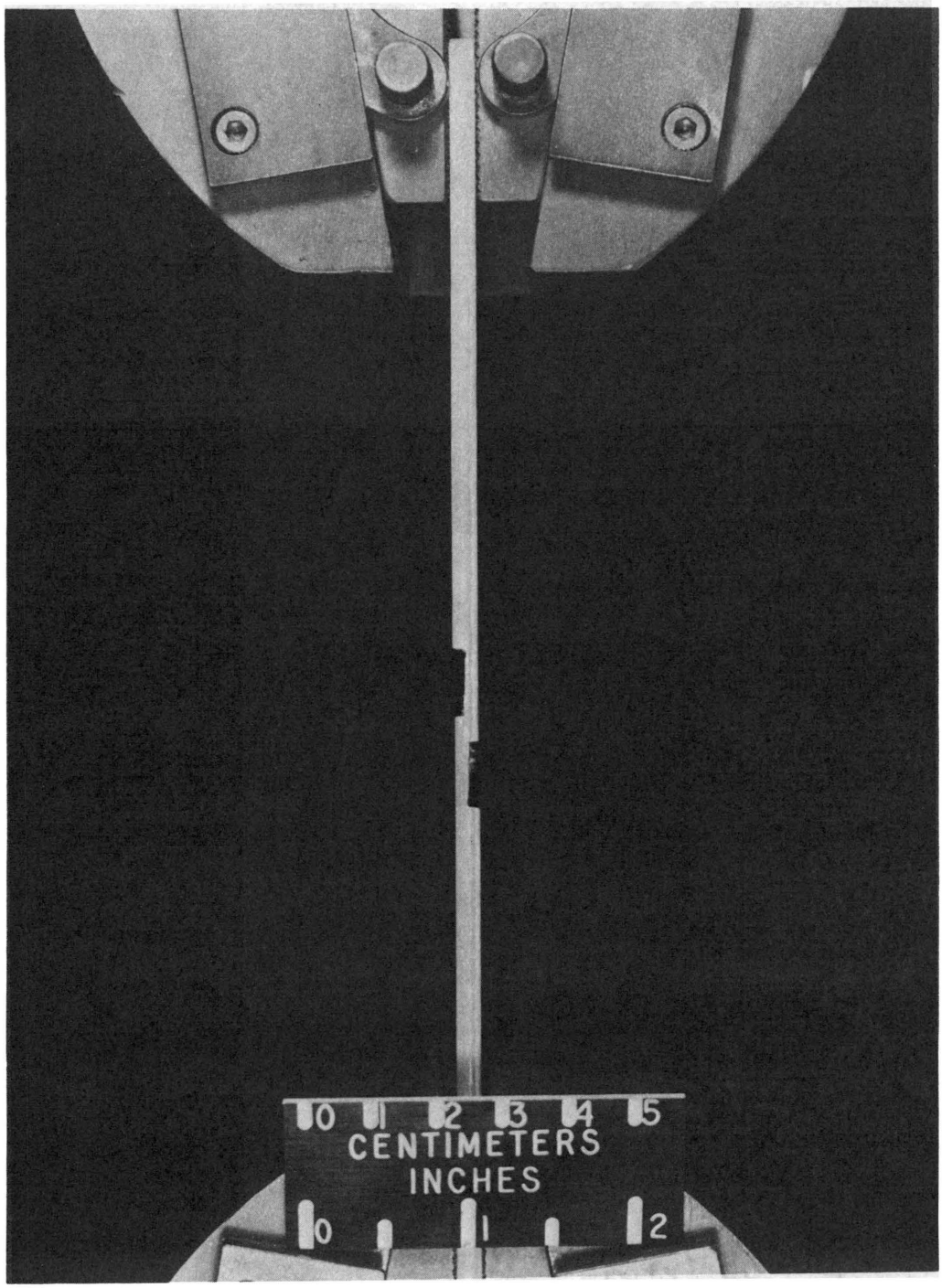

(c) After failure.

Figure 6.- Concluded.

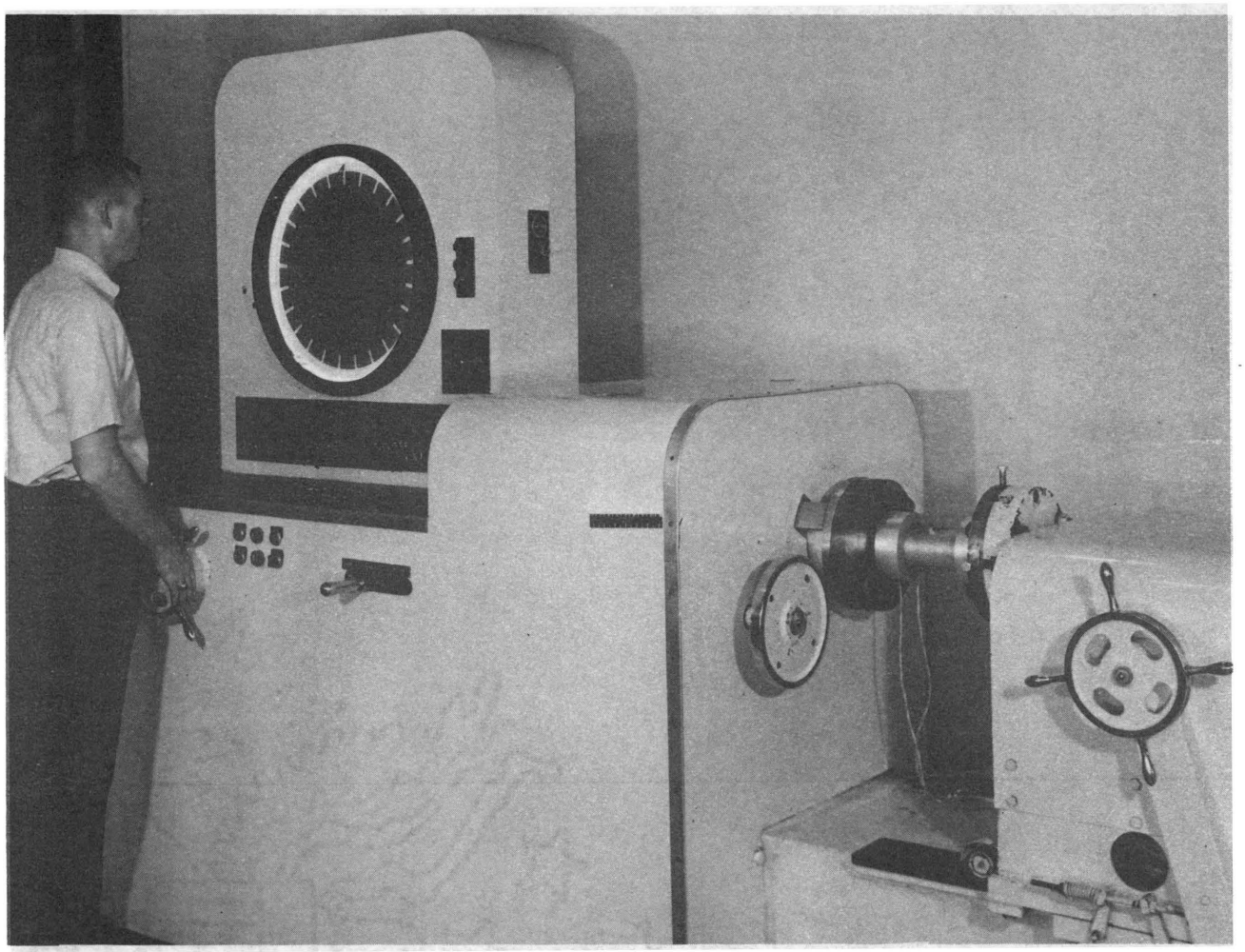

(a) Overall view.

Figure 7.- Torsion test apparatus for circumferentially wound cylinder.

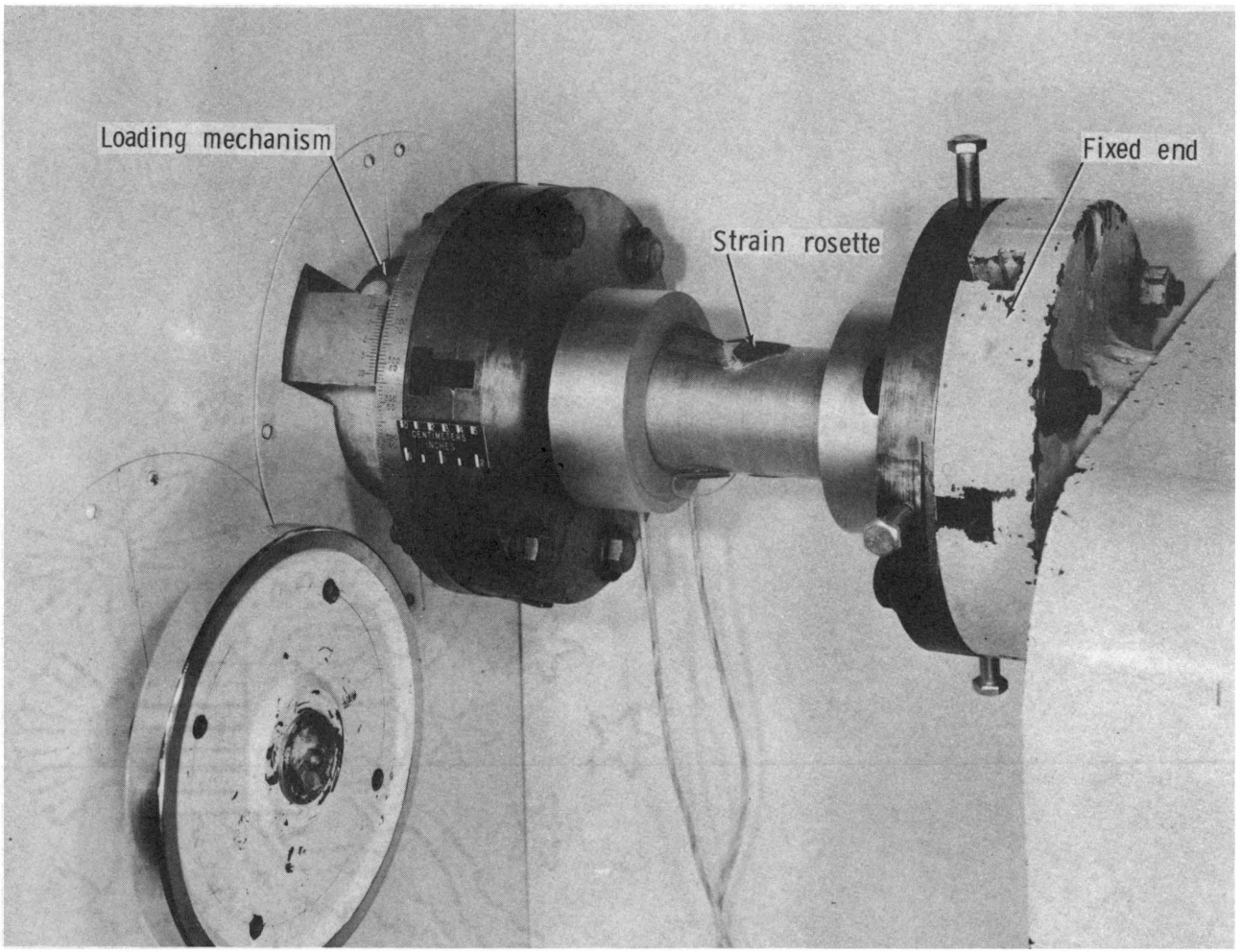

(b) Closeup view.

Figure 7.- Concluded.

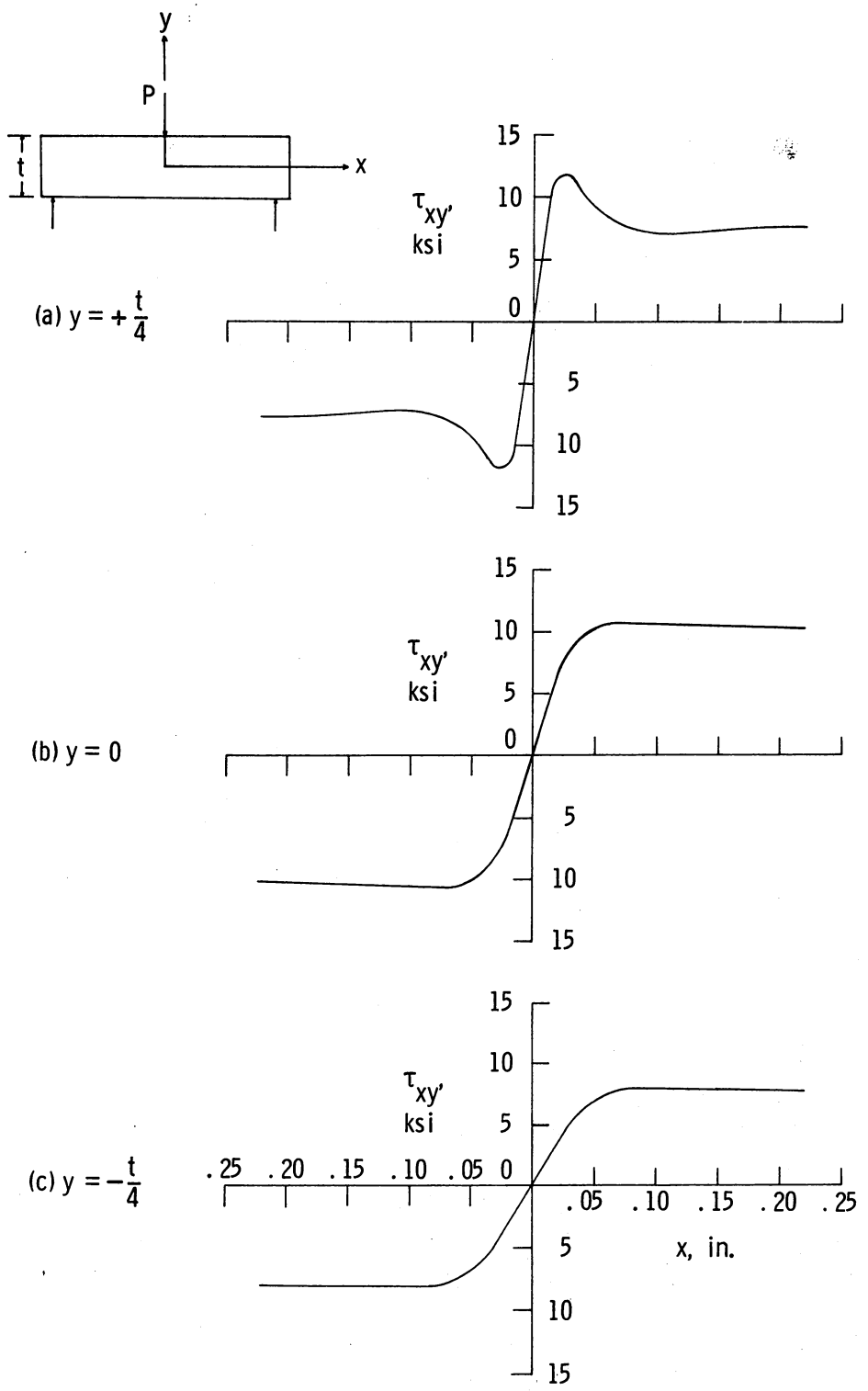

Figure 8.- Typical shear stress distribution for concentrated load on short beam.

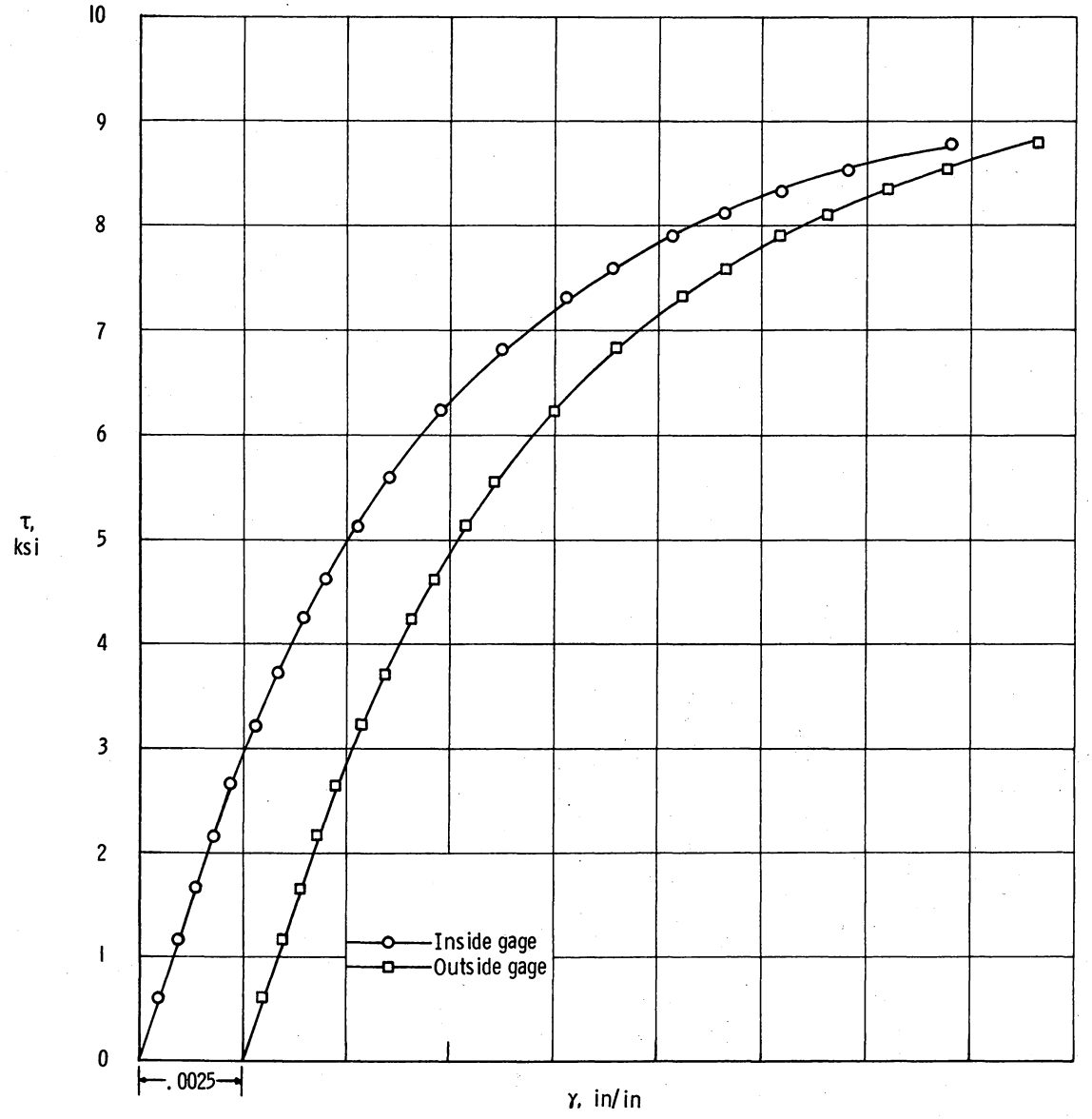

(a) Cylinder 1.

Figure 9.- Shear stress-strain curves for glass-epoxy circumferentially wound cylinders.

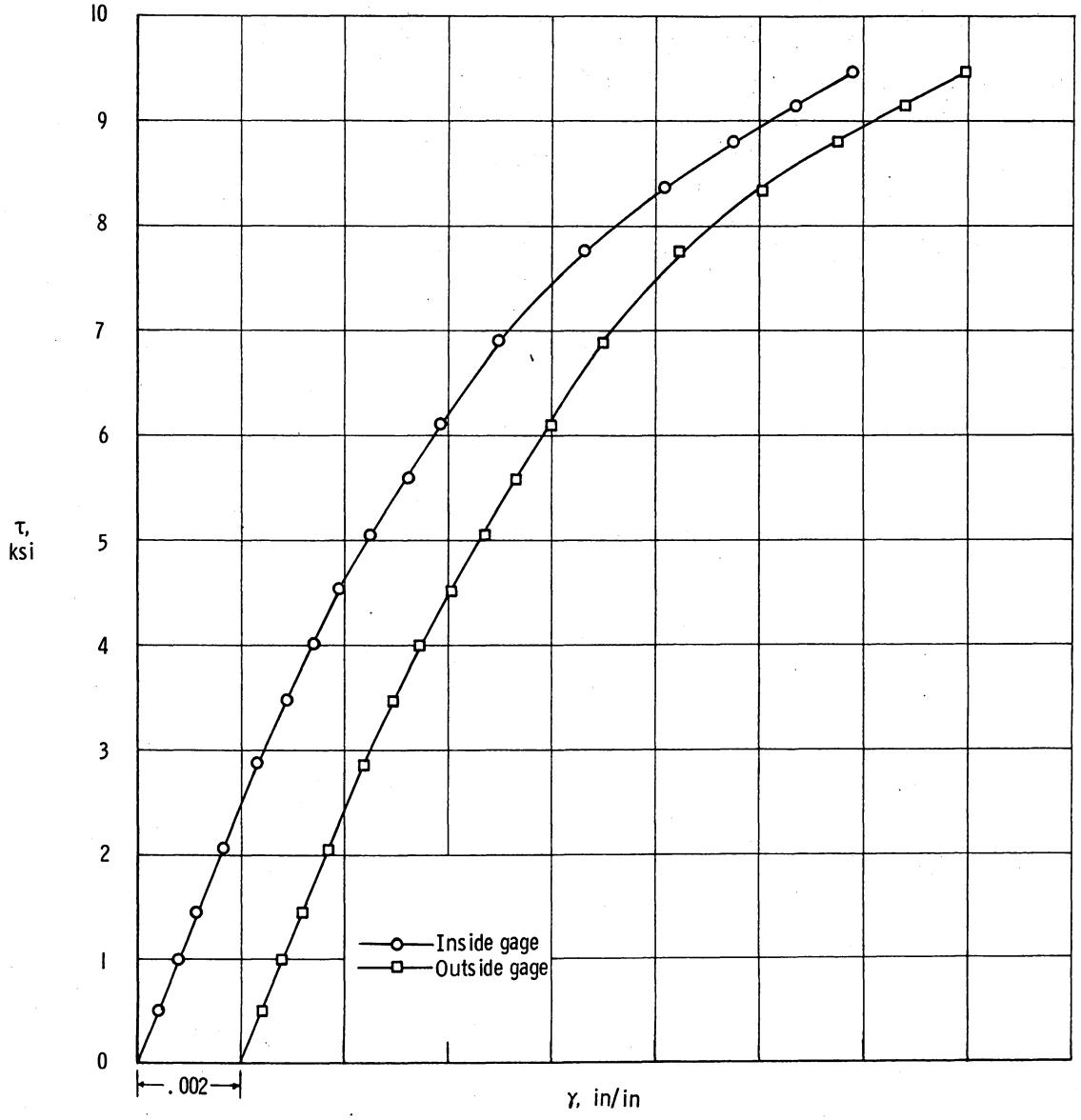

(b) Cylinder 2.

Figure 9.- Continued.

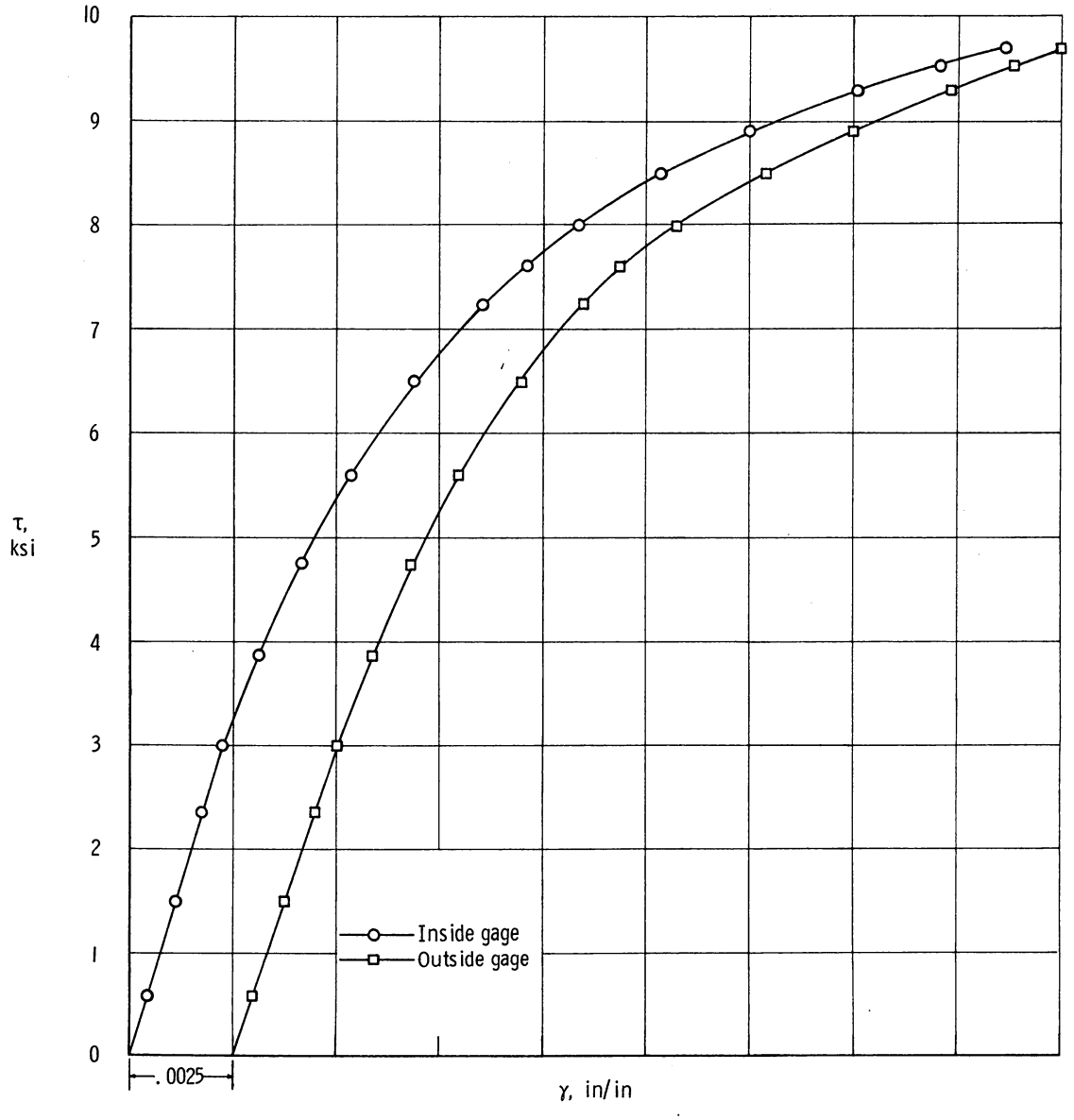

(c) Cylinder 3.

Figure 9.- Continued.

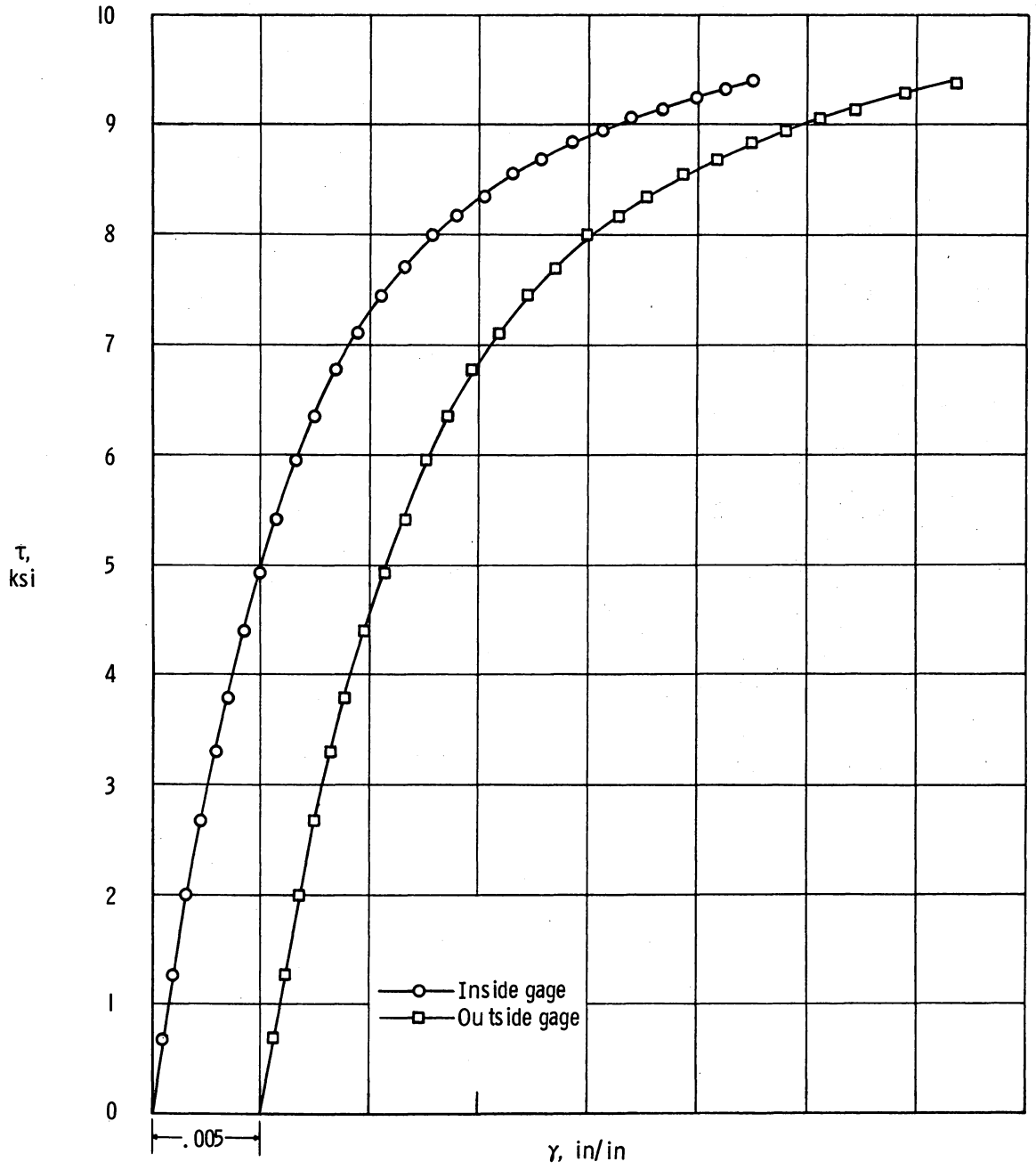

(d) Cylinder 4.

Figure 9.- Continued.

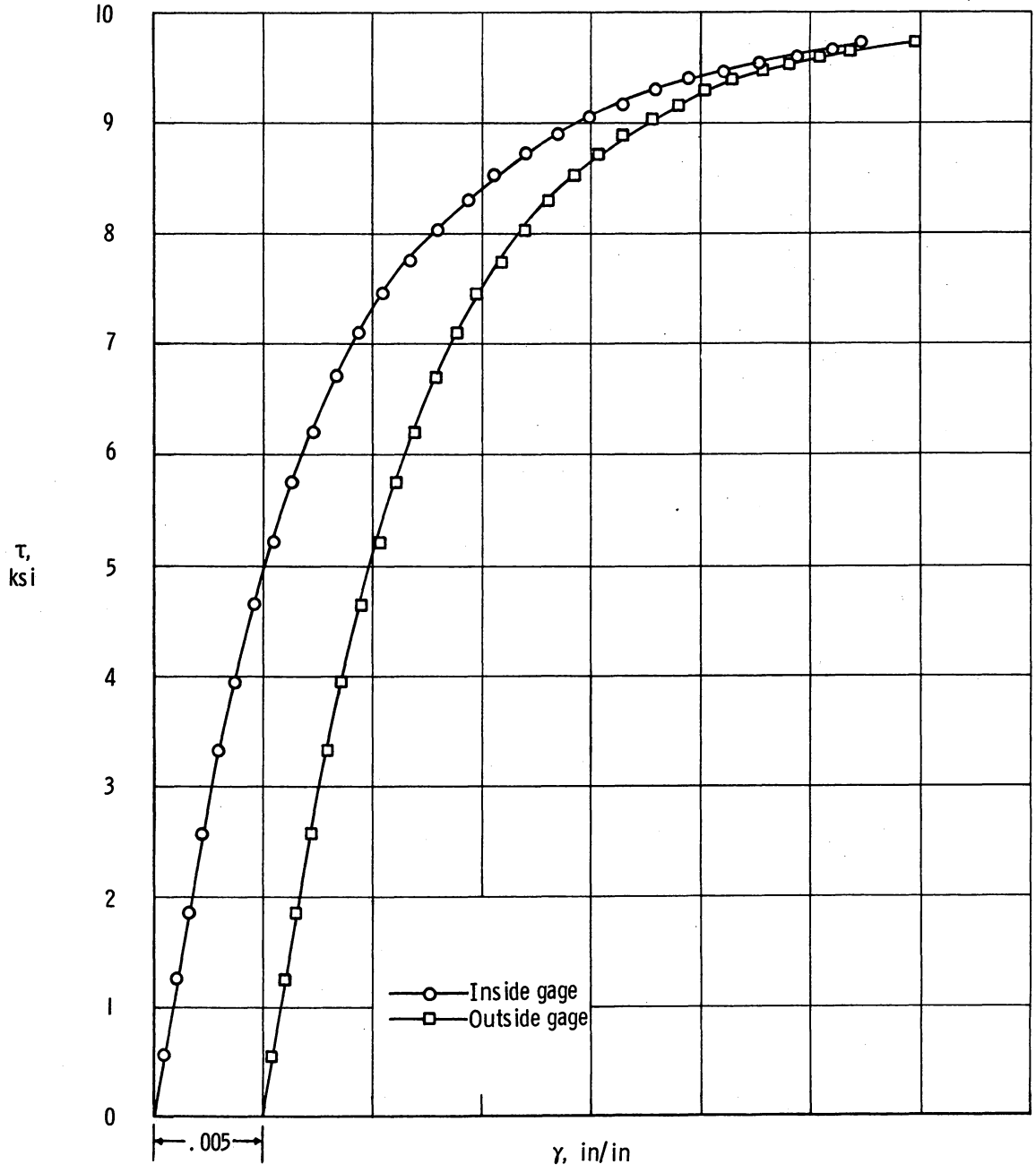

(e) Cylinder 5.

Figure 9.- Concluded.

CORRELATION OF THREE STANDARD SHEAR TESTS FOR UNIDIRECTIONAL GLASS-EPOXY COMPOSITES

By

H. Benson Dexter

ABSTRACT

The shear strength of unidirectional glass-epoxy composites was determined experimentally by three standard shear tests. The tests consisted of short beam interlaminar shear tests, saw-cut shear tests, and torsion tests on circumferentially wound cylinders. Test results show that the short beam interlaminar shear tests and the torsion tests of circumferentially wound cylinders give approximately the same maximum shear stress. Test results also showed that the saw-cut shear test is not a good interlaminar shear test because of stress concentrations at the base of the saw cuts and high tearing stresses normal to the plane of shear. The shear strength determined by the beam and torsion tests is approximately 10 ksi, whereas the average shear strength for the saw-cut specimens is approximately 2.5 ksi.